Mineralogical and Geochemical Characteristics of Trace Elements in the Yongdingzhuang Mine, Datong Coalfield, Shanxi Province, China

Yue Yuan [1,2,3], Shuheng Tang [1,2,3,*], Songhang Zhang [1,2,3] and Ning Yang [1,2,3]

[1] School of Energy Resources, China University of Geosciences (Beijing), Beijing 100083, China; yuanyue@cugb.edu.cn (Y.Y.); zhangsh@cugb.edu.cn (S.Z.); yangning@cugb.edu.cn (N.Y.)

[2] Beijing Key Laboratory of Unconventional Natural Gas Geological Evaluation and Development Engineering, China University of Geosciences, Beijing 100083, China

[3] Coal Reservoir Laboratory of National Engineering Research Center of CBM Development & Utilization, China University of Geosciences, Beijing 100083, China

[*] Correspondence: tangsh@cugb.edu.cn; Tel.: +86-10-8232-2005

Abstract: Fifteen samples of No. 4 coal from the Yongdingzhuang Mine in Datong Coalfield were tested for their elemental compositions, modes of occurrence, and mineralogical compositions, using X-ray powder diffraction, X-ray fluorescence spectrometry, inductively coupled plasma mass spectrometry, and scanning electron microscopy equipped with an energy-dispersive X-ray spectrometer. The samples have low sulfur content (0.63%). The major minerals are kaolinite and quartz, followed by pyrite and anatase. Compared with averages for the Chinese coals, the percentages of SiO_2 (15.11%), TiO_2 (0.7%), and Al_2O_3 (10.39%) are much higher. In No. 4 coals, Li (62.81 µg/g), Be (6.94 µg/g), Zr (235 µg/g), Ga (17.04 µg/g), F (165.53 µg/g), Tl (1.93 µg/g), and Hg (0.34 µg/g) are some potentially valuable and toxic trace elements with higher concentrations than Chinese coals and World hard coals. Lithium and F mainly have kaolinite associations. With the exception of kaolinite, Li, and F also partly occur in anatase, gorceixite and goyazite. Beryllium largely occurs in anatase; gallium is mainly associated with kaolinite and to a lesser extent, with gorceixite and goyazite; zirconium is associated with kaolinite, gorceixite and goyazite; and thallium and Hg occur in in pyrite. Potentially valuable elements (including Al, Li, Ga, and Zr) might be recovered as value-added byproducts from coal ash. Toxic elements (e.g., Be, F, Tl, and Hg) might have potential adverse effects to the environment and human health during coal processing. In addition, the distribution patterns of rare earth elements and yttrium (REY) indicate that the REY in No. 4 coals originated from the granite of Yinshan Oldland, and natural waters or hydrothermal solutions that may circulate in coal basins.

Keywords: trace elements; minerals; mode of occurrence; Datong coalfield

1. Introduction

China is the major consumer of coal worldwide, accounting for 50% of the total annual world coal consumption [1] and coal utilization will continue to play a leading role in energy consumption in the future [2]. Due to potentially hazardous compositions of coal, both the environment and human health are tremendously threatened by the pollution generated through both coal production and utilization [3,4]. In recent decades, an increasing number of studies have focused on relevant studies [5–7], detailing the abundances, elemental compositions, and occurrence modes of various trace elements in coal, including toxic (e.g., F, As, Hg, and Pb) [8,9] and valuable elements (e.g., Ge, Ga, Al, Nb, Zr, and rare earth elements) [10–12]. The trace elements can provide not only geologic information

about depositional conditions of coal, coal-bearing sequences, and regional tectonic history [13–15], but also practical information for potential industrial utilization of rare metals (e.g., Ge, Ga, and Al) which can be industrially utilized if they are enriched to the levels exceeding economic grades [16,17].

The Datong Coalfield is one of the largest coal producers of China and is located in northern Shanxi Province, which is adjacent to Shaanxi Province, Hebei Province, and the Inner Mongolia Autonomous Region (Figure 1). Many studies have been conducted on the geochemical characteristics of the Ordos Basin and the Ningwu Basin, which are adjacent to the Datong Coalfield [18,19]. However, few previous studies have been carried out about the geochemical characteristics on the coals in the Datong Coalfield. This paper primarily reports the mineralogical compositions, geochemical characteristics and origin of the trace elements from the Yongdingzhuang Mine in the Datong Coalfield. In order to investigate the potential for industrial utilization of the valuable elements and potential threats of the toxic elements, this paper also focuses on the concentrations and modes of occurrence of these valuable and toxic elements [20].
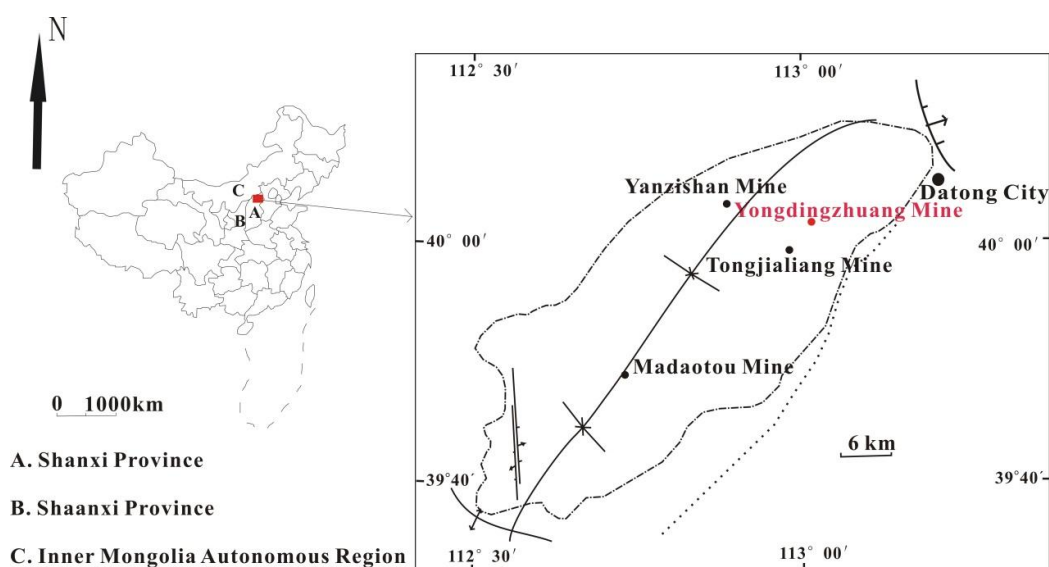

Figure 1. Location map of both the Datong Coalfield and the Yongdingzhuang Mine [18].

2. Geological Setting

The Datong Coalfield is located to the south of the Yinshan Oldland and stretches 50 km long (N-S) and 30 km wide (W-E), covering a total area of 1900 km^2 [21]. It is bound to the west by the Pingwang-Emaokou fault, to the east by the Lvliang mountain syncline, and to the north by the Hongtao mountain syncline. Due to Caledonian tectonic movement, the Ordovician Majiagou Formation has been extensively weathered, leading to erosion of the Upper Ordovician, the Silurian, Devonian, and the Lower Carboniferous strata. The coals in the Datong Coalfield began to accumulate sediments during the Late Palaeozoic in part of the North China Craton. Consequently, the strata were assigned to the Benxi, Taiyuan, Shanxi, Shihezi, and Shiqianfeng Formations. The faults in the northern coalfield provided channels for magma intrusion. The lamprophyre intrusions, which occurred during the Indosinian epoch in the north of the coalfield, resulted in thermal contact metamorphism and silicification between coal seams [21].

The Shanxi Formation has a total thickness of 20–80 m and is mainly composed of conglomerate, sandstone, siltstone, mudstone, and four coal seams identified as Nos. 1, 2, 3, and 4 coal, respectively, from top to bottom. The thickness of the coal seams ranges between 0.16 and 10.63 m (Figure 2). According to previous research, the Shanxi Formation was deposited in fluvial facies [22].
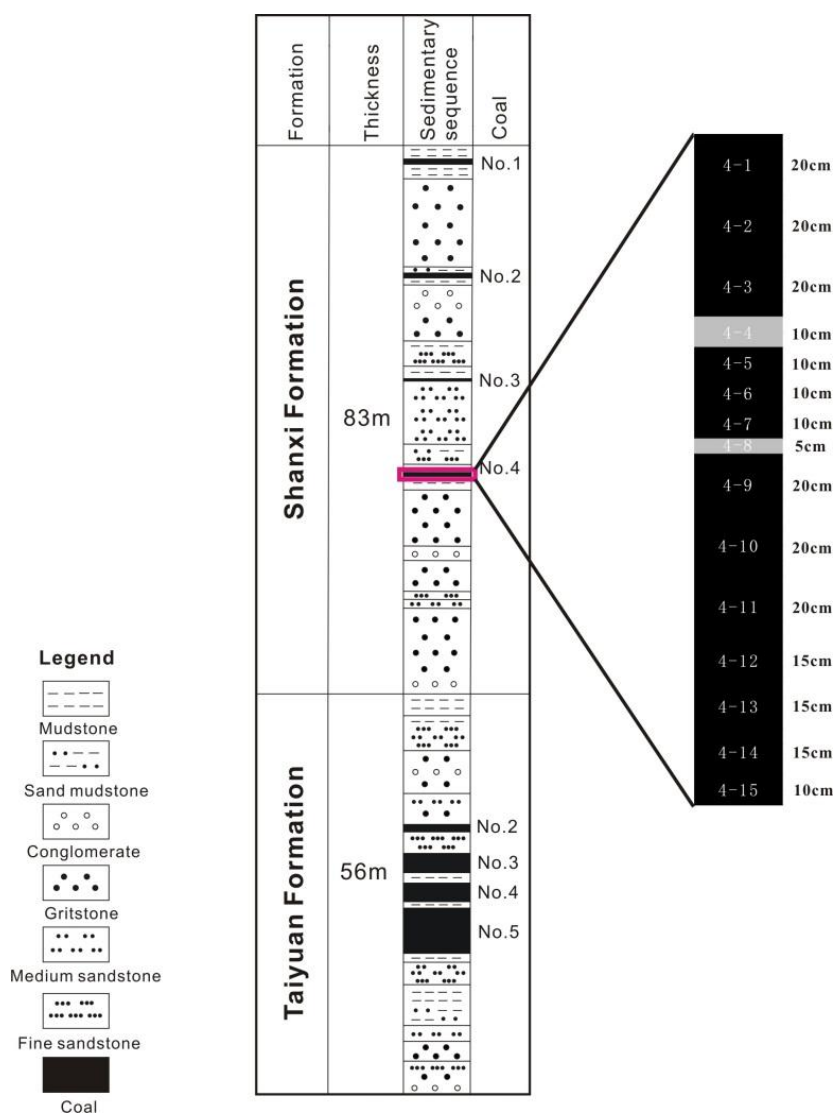
Figure 2. General stratigraphic sequence of the Datong Coalfield.

3. Samples and Methods

Fifteen samples, consisting of two partings and 13 coal benches with a total thickness of 1.15 m from top to bottom, were collected from No. 4 coal in the Yongdingzhuang Mine following the Chinese Standard Method GB 482-2008 [23]. The samples were cut into sections of 10 cm width and 10 cm depth and immediately stored in plastic bags to prevent contamination and oxidation. All samples were ground to 80-mesh and 200-mesh prior to geochemical analysis.

The 80-mesh samples were used to analyze both the mineralogical composition and distribution. The mineralogical composition was determined via microscopy (Leica DM 2500P microscope by Leica Microsystems, Solms, Germany). A scanning electron microscope (HITACHI UHR FE-SEM, SU8220, HITACHI, Tokyo, Japan) equipped with an energy-dispersive X-ray spectrometer (SEM-EDS, HITACHI, Tokyo, Japan) was used to study the mineral distribution of the coal and the distribution patterns of several elements of interest.

Low-temperature ashes were used for the 200-mesh samples and performed on an EMITECH K1050 plasma asher (Quorum, Ashford, UK), with the temperature maintained below 150 °C. X-ray diffraction (XRD, Rigaku, Tokyo, Japan) analyses on the low-temperature ashes were performed via

Ni-filtered Cu-Kα radiation and a scintillation detector. XRD patterns were recorded over a 2θ interval from 10° to 70°, at a step size of 0.01°.

All 200-mesh samples were ashed at a temperature of 815 °C and the residues were used to determine the concentrations of major-element oxides (SiO_2, TiO_2, Al_2O_3, Fe_2O_3, MgO, CaO, MnO, Na_2O, K_2O, and P_2O_5) by X-ray fluorescence spectrometry (XRF) (Thermo ADVANT XP+, Thermo Fisher, Waltham, MA, USA). Trace elements, including REY, except for As, Se, Hg, and F, were determined via inductively coupled plasma mass spectrometry (ICP-MS) [24]. For ICP-MS, 200-mesh samples were digested using an UltraClave Microwave High Pressure Reactor (Milestone, Sorisole, Italy). The basic load for the digestion tank was composed of 330 mL distilled H_2O, 30 mL 30% H_2O_2, and 2 mL 98% H_2SO_4. The initial nitrogen pressure was set to 50 bars and the highest temperature was set to 240 °C, which lasted for 75 min. The reagents for the 50 mg sample digestion were 5 mL 40% HF, 2 mL 65% HNO_3, and 1 mL 30% H_2O_2. Multi-element standards (Inorganic Ventures: CCS-1, CCS-4, CCS-5 and CCS-6) were used for the calibration of trace element concentrations [24]. Arsenic and Se were analyzed via ICP-MS with collision/reaction cell technology (ICP-CCT-MS) [25]. Fluorine was determined via pyrohydrolysis combined with an ionselective electrode (ISE) based on the ASTM method [26]. Mercury was determined using a Milestone DMA-80 Hg analyzer (Milestone, Sorisole, Italy) [27].

4. Results

4.1. Proximate Analysis

Bench thickness, forms of sulfur and proximate analysis of the No. 4 coal seam of the Yongdingzhuang Mine are listed in Table 1.

Table 1. Bench thickness (cm), proximate, and forms of sulfur (%) of No. 4 coal samples from the Yongdingzhuang Mine.

Sample	Thickness (cm)	M_{ad}	A_d	V_{daf}	$S_{t.d}$	$S_{p.d}$	$S_{s.d}$	$S_{o.d}$
YDZ4-1	20	1.7	14.47	33.43	1.35	0.96	0.01	0.38
YDZ4-2	20	1.56	13.6	31.16	0.51	0.30	0.01	0.19
YDZ4-3	20	1.84	9.82	30.61	1.10	0.74	0.01	0.35
YDZ4-4	10	0.74	83.19	18.35	0.10	0.09	0.01	0.00
YDZ4-5	10	1.66	12.9	35.94	0.62	0.18	0.01	0.43
YDZ4-6	10	1.29	48.67	16.07	0.18	0.16	0.01	0.01
YDZ4-7	10	1.28	39.3	24.13	0.20	0.18	0.01	0.01
YDZ4-8	5	0.95	61.21	19.43	0.20	0.17	0.01	0.02
YDZ4-9	20	1.28	27.46	28.53	0.43	0.20	0.01	0.21
YDZ4-10	20	1.55	12.43	26.87	1.02	0.20	0.01	0.80
YDZ4-11	20	1.39	11.89	25.68	1.97	0.31	0.02	1.65
YDZ4-12	15	1.36	20.23	23.92	0.56	0.15	0.01	0.40
YDZ4-13	15	1.31	19.58	21.68	0.37	0.33	0.01	0.03
YDZ4-14	15	1.33	20.55	21.89	0.35	0.25	0.01	0.09
YDZ4-15	10	1.55	12.51	32.14	0.53	0.34	0.01	0.18
AVE	-	1.46	20.76	27.45	0.70	0.33	0.01	0.36

M, moisture; A, ash yield; V, volatile matter; ad, air-dry basis; d, dry basis; daf, dry and ash-free basis; S_t, total sulfur; S_p, pyritic sulfur; S_s, sulfate sulfur; S_o, organic sulfur.

The No. 4 coals from Yongdingzhuang Mine are considered as a medium ash coal, with an average ash yield value of 20.76% (ranging from 9.82% to 48.67%), according to the Chinese National Standard (GB/T15224.1-2010, 2011, 10.0–20.00% for low ash coal, 20.0–30.00% for medium ash coal, and 30.0–40.00% for high ash coal) [28].

The moisture content of No. 4 coals ranges from 0.95% to 1.84%, averaging 1.46%, indicating that No. 4 coals are low moisture coals in accordance with the MT/T 850–2000 [29] (<5% for low moisture coal, 5% to 15% for medium moisture coal, and >15% for high moisture coal).

The volatile matter content of No. 4 coal seam ranges from 16.07% to 35.94%, with a mean of 27.45% suggesting that this coal is a medium volatile coal according to the MT/T 849-2000 [30] (20.01–28.00% for medium volatile coal, 28.01–37.00% for medium-high volatile coal, 37.01–50.00% for high volatile coal, and >50.01% for super high volatile coal).

The No. 4 coals are considered as low sulfur coals, with total sulfur contents ranging from 0.18% to 1.97%, averaging 0.70%, based on the Chinese National Standard (GB/T 15224.2-2010, 2011) [31] (<0.5% for ultra-low sulfur coal, 0.51–0.9% for low sulfur coal, and 0.9–1.50% for medium sulfur coal). Total sulfur consists of inorganic sulfur (including pyritic sulfur, 0.15–0.96%, 0.33% on average; sulfate sulfur, 0.01–0.02%, 0.01% on average) and organic sulfur (0.01–1.65%, 0.36% on average).

In summary, the No. 4 coals of the Yongdingzhuang Mine are characterized by medium ash, low moisture, medium volatile, and low sulfur coals.

4.2. Mineralogical Composition

The mineralogical composition of the coal samples from No. 4 coal of the Yongdingzhuang Mine is primarily characterized by kaolinite and quartz and, to a lesser extent, by pyrite and anatase, based on the SEM-EDS and XRD analyses (Figure 3).
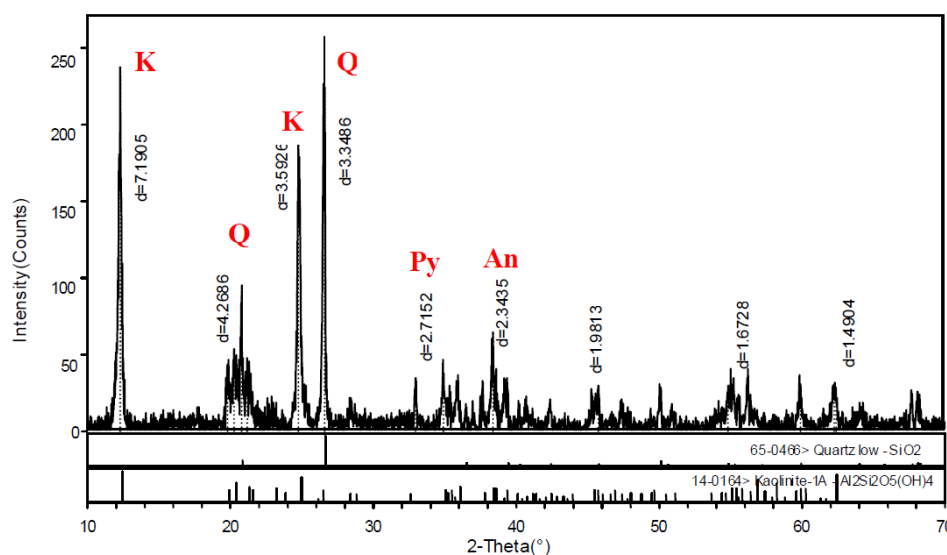

Figure 3. X-ray diffraction (XRD) pattern of coal sample YDZ4-11 K, Kaolinite; Q, Quartz; Py, Pyrite; An, Anatase.

Clay minerals are commonly detected in coals, including kaolinite, illite, chlorite and montmorillonite. Based on both XRD and SEM-EDS, kaolinite was found to be the most abundant mineral and mainly occurs as lumps and infillings of macerals (Figure 4A,B). Two main occurrences of kaolinite have been found in samples, one as disseminated particles in collodetrinite and the other as cell-fillings in fusinite. Filling fusinite indicates that kaolinite may indicate formation via authigenic processes (Figure 4A) [32]. Part of the kaolinite shows dissemination in collodetrinite, which is suggestive of a syngenetic origin (Figure 4B) [32,33].

Quartz is distributed as detrital grains in macerals throughout samples, along with vein quartz in coals (Figure 4C). Detrital grains with round edges have a terrigenous detrital origin, indicating transportation over a long distance from the sediment source region (Figure 4D) [34,35]. Furthermore, epigenetic quartz predominately occurs as vein quartz.
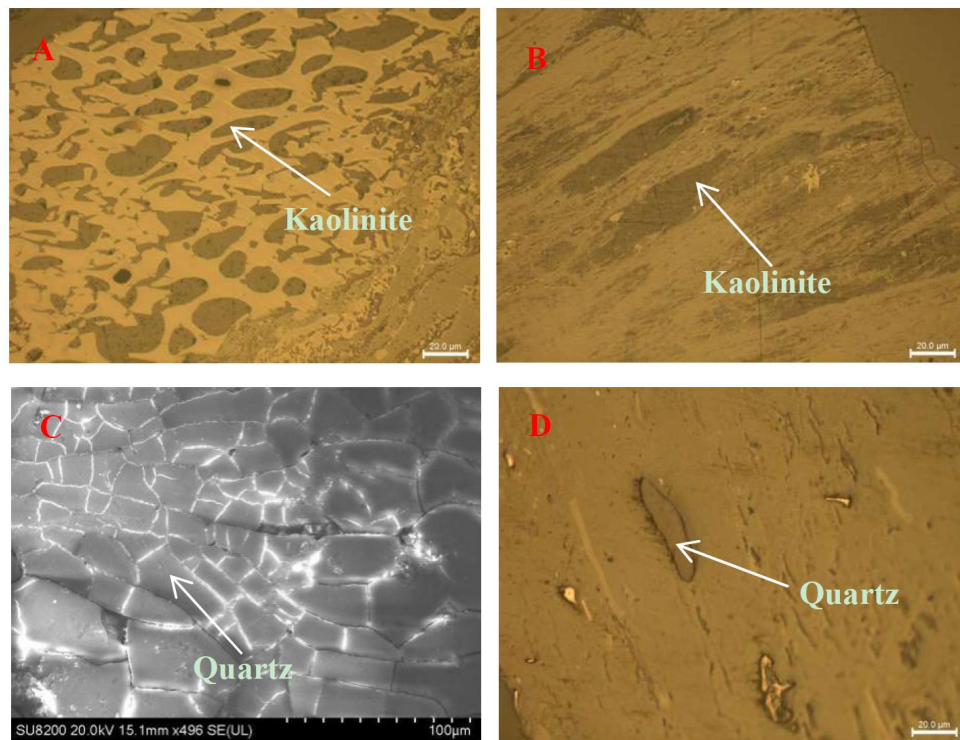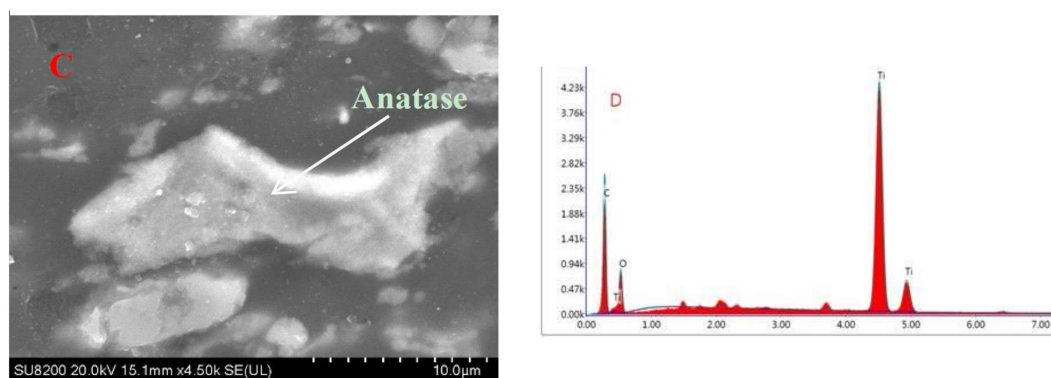
Figure 4. Kaolinite and quartz in the No. 4 coal. (**A**) Kaolinite in fusinite (reflected light) (500×); (**B**) kaolinite in collodetrinite (reflected light) (500×); (**C**) crystalline quartz (SEM, secondary electron image); (**D**) quartz in collodetrinite (reflected light) (500×).

Pyrite mainly occurs as fracture-filling and discrete crystals in No. 4 coals. It can be deduced that discrete crystals are related to a syngenetic origin (Figure 5A) [36]. However, fracture-filling pyrite was deposited from migrating solutions, after compaction of the peat into coals, suggesting an epigenetic origin (Figure 5B) [37]. Anatase occurs as detrital grains in collodetrinite, indicating a syngenetic origin (Figure 5A,B) [36,38].
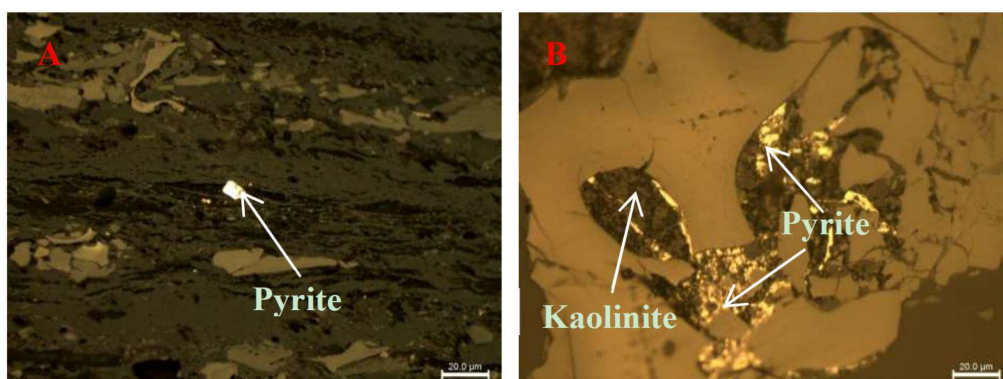
Figure 5. *Cont.*

Figure 5. Pyrite and anatase in coals. (**A**) Pyrite in collodetrinite (oil immersion reflected light) (500×); (**B**) pyrite in fusinite (reflected light) (500×); (**C**) crystalline anatase (SEM, secondary electron image); and (**D**) energy dispersive X-ray spectrometry (EDS).

4.3. Geochemistry

4.3.1. Major Elements

The concentrations of major oxides in the No. 4 coals are listed in Table 2, including average values, LOI (loss on ignition), and concentration coefficients (CC = the ratio of an average elemental concentration in the investigated coal/the average concentrations for either world coals or Chinese coals) [38]. The concentrations for major oxides are as follows: SiO_2 (11.14%), Al_2O_3 (7.16%), TiO_2 (0.67%), Fe_2O_3 (0.60%), MgO (0.03%), K_2O (0.03%), CaO (0.10%), P_2O_5 (0.01%), Na_2O (0.0028%), and MnO (0.0008%).

Table 2. Concentration of major oxides in No. 4 coal (%) (Recalculated from the dry ash basis to the whole-coal basis).

Sample	LOI	SiO_2	TiO_2	Al_2O_3	Fe_2O_3	MgO	CaO	MnO	Na_2O	K_2O	P_2O_5	SiO_2/Al_2O_3
YDZ4-1	85.53	7.49	0.18	4.57	1.28	0.07	0.29	0.0032	0.0048	0.02	0.013	1.64
YDZ4-2	86.4	6.52	0.17	5.00	1.18	0.07	0.26	0.0014	0.0021	0.04	0.006	1.30
YDZ4-3	90.18	6.12	0.16	3.08	0.14	0.03	0.12	0.0011	bdl	0.01	0.004	1.99
YDZ4-4	16.81	48.54	0.80	32.27	0.50	0.12	0.09	0.0012	0.0073	0.62	0.061	1.50
YDZ4-5	87.1	7.00	0.12	5.34	0.23	0.02	0.05	0.0003	0.0002	0.03	0.005	1.31
YDZ4-6	51.33	27.00	1.66	19.39	0.26	0.02	0.06	bdl	0.0067	0.07	0.035	1.39
YDZ4-7	60.7	21.73	0.98	15.98	0.32	0.02	0.06	0.0007	0.0095	0.05	0.044	1.36
YDZ4-8	38.79	33.35	1.00	26.11	0.26	0.02	0.07	bdl	0.0103	0.06	0.024	1.28
YDZ4-9	72.54	14.76	0.39	11.65	0.35	0.02	0.09	0.0005	0.0059	0.04	0.013	1.27
YDZ4-10	87.57	6.10	0.15	4.93	0.97	0.02	0.09	0.0002	0.0022	0.01	0.004	1.24
YDZ4-11	88.11	5.30	0.27	4.07	2.08	0.01	0.05	0.0004	0.0025	0.01	0.005	1.30
YDZ4-12	79.77	12.00	1.33	6.22	0.45	0.01	0.05	0.0009	bdl	0.03	0.014	1.93
YDZ4-13	80.42	11.67	1.40	6.10	0.21	0.01	0.05	0.0005	bdl	0.02	0.013	1.91
YDZ4-14	79.45	12.49	1.38	6.25	0.22	0.01	0.05	0.0006	bdl	0.02	0.013	2.00
YDZ4-15	87.49	6.60	0.58	4.96	0.17	0.01	0.05	0.0002	0.0020	0.02	0.006	1.33
AVE	79.74	11.14	0.67	7.16	0.60	0.03	0.10	0.0008	0.0028	0.03	0.01	1.54
Chinese coal [1]	-	8.47	0.33	5.98	4.85	0.22	1.23	0.015	0.16	0.19	0.09	1.42
CC	-	1.32	2.03	1.20	0.12	0.14	0.08	0.05	0.02	0.16	0.11	-

LOI, loss on ignition; [1], Dai, et al. (2012) [20]; nd, not detected; bdl, below detected limit; CC, concentration coefficients between Chinese coal and No. 4 coal.

Compared with the average values for Chinese coals [20], TiO_2 is slightly enriched (2 < CC < 5) in No. 4 coals, while the Al_2O_3 and SiO_2 concentrations are close to the average Chinese coal values (0.5 < CC < 2). The remaining major oxides are depleted (CC < 0.5). In general, Al_2O_3 and SiO_2 are the most abundant element oxides in all samples. The ratios of the SiO_2/Al_2O_3 range from 1.24 to 2.00 (average 1.54), which are higher than those of average Chinese coal (1.42) [20] and the theoretical ratio

of kaolinite (1.18). This is due to the relatively high concentration of free silicon in the coal, which was mainly found in the form of quartz [39,40].

4.3.2. Trace Elements

The concentrations of 32 trace elements determined in the No. 4 coal seam samples from the Yongdingzhuang Mine are listed in Table 3, along with the CC values.

Based on the enrichment classification of Dai et al. [38] and compared with the corresponding averages for world hard coals [41], only Zr (235 µg/g) is enriched, showing a CC value above 5 (CC = 6.53). Fluorine (CC = 1.51), V (CC = 1.12), Cr (CC = 1.55), Ni (CC = 1.58), Zn (CC = 1.21), As (CC = 0.76), W (CC = 1.48), and U (CC = 1.84) are relatively close to the world hard coal values (0.5 < CC < 2). Rubidium (CC = 0.06), Sr (CC = 0.11), Cs (CC = 0.15), Ba (CC = 0.40), and Bi (CC = 0.44) are depleted. The concentrations of the remaining trace elements are slightly elevated (2 < CC < 5) (Figure 6A).

Compared to average Chinese coals [20], Be (CC = 3.29), Sc (CC = 2.06), Cu (CC = 2.94), Ga (CC = 2.40), As (CC = 2.28), Zr (CC = 2.63), Zn (CC = 2.78), Sb (CC = 3.64), W (CC = 2.37), Hg (CC = 2.30), Tl (CC = 4.62), Pb (CC = 2.02), and Th (CC = 3.78) are slightly enriched in the investigated coals. Rubidium (CC = 0.12), Sr (CC = 0.08), Cs (CC = 0.14), Cd (CC = 0.44), and Ba (CC = 0.37) are depleted and the remaining elements are similar to those of average Chinese coals (Figure 6B). Note that almost all the trace elements have higher concentrations in partings (YDZ4-4 and YDZ4-8) than those in coal benches.
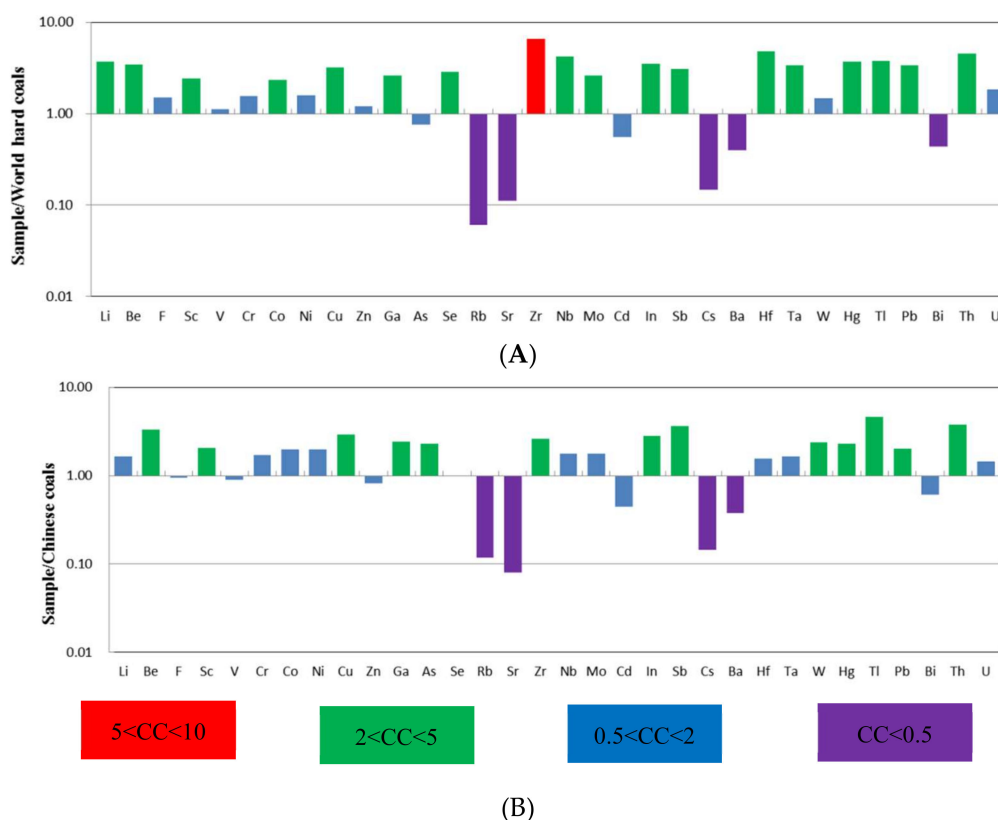
Figure 6. Concentration coefficients of trace elements in No. 4 coal; (**A**) normalized by average concentrations in the world hard coals; (**B**) normalized by the average concentration in the Chinese coals.

5. Discussion

5.1. Elemental Associations

Affinity and cluster analyses among elements are effective indirect methods to analyze elemental modes of occurrence [42,43]. Correlation of the element concentrations with ash yield may provide preliminary information on their organic or inorganic affinities [44]. In this paper, all elements were classified by the correlation between their ash yields and elemental concentrations, demonstrating either inorganic or organic affinity (Figure 7). All of these elements were then divided into five groups according to their correlation coefficients with their ash yields [45].

Group 1 includes Na_2O, Al_2O_3, SiO_2, P_2O_5, K_2O, Li, F, Sc, Rb, Nb, In, Cs, Ba, Hf, Ta, Bi, Th, and U, all of which have a strong correlation with the ash yield (r_{ash} = 0.7–1.0). The correlation coefficients between ash yield as well as Al_2O_3 and SiO_2 are 0.99 and 1.00, respectively, indicating silicate and aluminosilicate associations (especially clay minerals) as major minerals in the coal samples. Additionally, Li, F, Sc, Rb, Nb, In, Cs, Ba, Hf, Ta, Bi, Th, and U also show high correlation coefficients with Al_2O_3 and SiO_2 (Table 4), indicating an aluminosilicate affinity (mainly in kaolinite). Moreover, Li, F, Sc, Rb, Cs, In, Ba, Bi, and Th have a strong correlation (r > 0.7) with P_2O_5 (Table 4), which is likely due to phosphate affinity [27,46].

Table 3. Concentrations of trace elements in the No. 4 coal from the Yongdingzhuang Mine (µg/g) (on whole-coal basis).

| Elements	Li	Be	F	Sc	V	Cr	Co	Ni	Cu	Zn	Ga	As	Se	Rb	Sr	Zr
YDZ4-1	21.27	3.84	92	8.15	26.10	34	31.10	64.20	52.30	34.30	16.90	24.33	2.47	0.80	11.60	306
YDZ4-2	12.50	5.53	77	9.01	17.40	28.10	16.40	30.20	57.40	26.60	13.40	1.71	2.87	0.68	9.40	182
YDZ4-3	7.91	2.39	96	5.08	19.80	14.90	17.90	27.60	46.30	21.10	18.20	15.07	1.32	1.16	9.46	267
YDZ4-4	90.60	2.83	550	5.93	24.50	48.60	4.37	25.90	18.20	20.80	25.20	1.29	1.47	24.90	116	152
YDZ4-5	20.60	2.76	96	4.91	36	14	20.50	26.40	58.20	27.70	22	1.53	3.94	1.22	9.60	355
YDZ4-6	192	8.30	267	17	50.80	37.30	2.40	24.40	58.30	31	31.20	1.68	5.42	2.86	12.50	330
YDZ4-7	145	7.44	248	16	37.30	24.90	1.88	14.10	34	24.40	18.80	0.82	3.13	1.87	18.50	268
YDZ4-8	174	6.15	327	9.26	29.50	14.20	2.79	14.10	18.40	22.80	26.30	1.02	2.40	1.88	10.80	218
YDZ4-9	85.60	4.83	168	7.53	23.80	13.70	10.80	18.90	47.30	29.20	13.20	1.58	2.99	1.36	11.50	200
YDZ4-10	26.70	5.23	83	4.67	15.10	15.80	16.90	24.70	16.90	12.70	7.16	8.68	2.87	0.34	2.86	108
YDZ4-11	17.80	5.75	68	4.03	17.90	21.20	27.40	29.30	53.40	28.10	10.10	18.52	2.38	0.30	9.26	151
YDZ4-12	38.80	10.80	100	10.20	36.30	38.20	8.73	22	54.40	39.20	10.80	3.40	3.68	1.18	13.60	191
YDZ4-13	42.20	13.20	152	12	51.30	47	8.49	24	72.70	54.90	13.50	1.73	6.55	0.92	15.20	242
YDZ4-14	38.30	11.80	96	11	45.80	41.40	7.98	21.90	61.10	57.50	13.80	1.83	5.90	0.71	12.80	238
YDZ4-15	28.80	8.33	63	7.83	31.10	11.40	11.90	22.30	56.80	53.50	15.70	1.37	4.74	0.82	8.12	217
AVE	52.11	6.94	123.54	9.03	31.44	26.30	14.03	26.92	51.47	33.86	15.75	6.33	3.71	1.09	11.11	235
World [1]	14	2	82	3.70	28	17	6	17	16	28	6	8.30	1.30	18	100	36
Chinese [2]	31.80	2.11	130	4.38	35.10	15.40	7.08	13.70	17.50	41.40	6.55	2.78	3.79	9.25	140	89.50
CC [3]	3.72	3.47	1.51	2.44	1.12	1.55	2.34	1.58	3.22	1.21	2.63	0.76	2.86	0.06	0.11	6.53
CC [4]	1.64	3.29	0.95	2.06	0.90	1.71	1.98	1.97	2.94	0.82	2.40	2.28	0.98	0.12	0.08	2.63
Elements	Nb	Mo	Cd	In	Sb	Cs	Ba	Hf	Ta	W	Hg	Tl	Pb	Bi	Th	U
YDZ4-1	13.10	11	0.14	0.08	1.40	0.08	34.30	5.29	0.41	1.33	0.79	4.65	30.90	0.24	8.07	3.52
YDZ4-2	5.57	7.42	0.08	0.10	0.92	0.06	32.80	3.86	0.39	1.26	0.12	0.62	14.50	0.31	8.24	2.17
YDZ4-3	9.20	12.70	0.12	0.10	0.98	0.19	37.50	5.60	0.33	2.44	0.86	5.27	31.50	0.28	7.79	3.22
YDZ4-4	31.40	1.80	0.08	0.17	12.30	3.05	326	5.70	2.96	3.04	0.17	0.47	32.60	1.63	26	3.54
YDZ4-5	12.80	8.34	0.15	0.12	1.13	0.17	34.20	8.27	0.42	1.14	0.31	0.77	56.10	0.28	10.20	5.11
YDZ4-6	44.80	3.76	0.16	0.27	0.43	0.63	143	9.79	2.99	3.03	0.08	0.22	50.90	1.40	30.80	6.98
YDZ4-7	22.70	2.19	0.13	0.20	0.34	0.32	124	7.50	1.69	1.59	0.05	0.10	60.10	0.97	23.90	4.64
YDZ4-8	26.20	1.31	0.11	0.16	0.27	0.28	180	8.51	1.61	2.22	0.08	0.24	39.50	0.46	15.20	4.29
YDZ4-9	8.08	1.93	0.10	0.14	0.52	0.17	72.10	6.20	0.53	0.79	0.21	0.76	26	0.22	10.40	3.17
YDZ4-10	3.50	7.11	0.06	0.07	0.42	0.03	20.80	2.41	0.23	0.42	0.46	2.91	19.80	0.17	5.09	1.49
YDZ4-11	4.63	5.64	0.10	0.13	8.46	0.03	25.20	3.35	0.35	0.73	1.17	9.82	13.20	0.26	5.25	1.40
YDZ4-12	23.40	2.68	0.09	0.12	0.32	0.14	77.60	5.03	1.39	1.61	0.22	1.21	18.20	0.43	21.80	3.36
YDZ4-13	25	2.79	0.10	0.17	10.20	0.10	72.20	6.53	1.69	1.83	0.18	0.56	25.60	0.59	25.20	3.93
YDZ4-14	29.50	2.40	0.11	0.20	9.07	0.07	65.10	6.91	2.09	2.19	0.18	0.54	26.60	0.59	24.70	3.86
YDZ4-15	16.90	3.50	0.10	0.11	5.61	0.12	34	4.69	0.77	0.73	0.15	0.78	23.90	0.50	7.37	2.69
AVE	16.86	5.50	0.11	0.14	3.06	0.16	59.45	5.80	1.02	1.47	0.37	2.17	30.56	0.48	14.52	3.50
World [1]	4	2.10	0.20	0.04	1.00	1.10	150	1.20	0.30	0.99	0.10	0.58	9	1.10	3.20	1.90
Chinese [2]	9.44	3.08	0.25	0.05	0.84	1.13	159	3.71	0.62	0.62	0.16	0.47	15.1	0.79	3.84	2.43
CC [3]	4.22	2.62	0.55	3.48	3.06	0.15	0.40	4.84	3.41	1.48	3.68	3.74	3.40	0.44	4.54	1.84
CC [4]	1.79	1.78	0.44	2.78	3.64	0.14	0.37	1.56	1.65	2.37	2.30	4.62	2.02	0.61	3.78	1.44

[1] Ketris and Yodvich (2009) [41]; [2] Dai et al. (2012) [20]; [3] CC = concentration in investigated coals/world hard coals; [4] CC = concentration in investigated coals/Chinese coals.

Table 4. Correlation coefficients between the concentration of each element in coal and ash yield or selected elements.

Correlation with Ash Yield
r_{ash} = 0.7–1.0: Na$_2$O (0.73) **, Al$_2$O$_3$ (0.99) **, SiO$_2$ (0.99) **, P$_2$O$_5$ (0.92) **, K$_2$O (0.88) **, Li (0.99) **, F (0.96) **, Sc (0.87) **, Rb (0.88) **, Nb (0.75) **, In (0.86) **, Cs (0.87) **, Ba (0.97) **, Hf (0.71) **, Ta (0.80) **, Bi (0.88) **, Th (0.77) **, U (0.74) ** r_{ash} = 0.4–0.69: TiO$_2$ (0.67) *, Ga (0.62) *, Sr (0.60) *, Cd (0.48), W (0.53), Pb (0.60) *, REY(0.68) r_{ash} = 0.2–0.39: Be (0.31), Cr (0.34), Se (0.36), Zr (0.36) r_{ash} = −0.2–0.19: MgO (−0.19), Cu (0.00), Zn (−0.01) r_{ash} < −0.2: Fe$_2$O$_3$ (−0.34), CaO (−0.27), MnO (−0.27), Co (−0.73) *, Ni (−0.34), As (−0.43), Mo (−0.55), Sb (−0.25), Hg (−0.54), Tl (−0.47)

Correlation with aluminosilicate
r_{Al-Si} = 0.7–1.0: P$_2$O$_5$, K$_2$O, Li, F, Sc, Rb, Nb, In, Cs, Ba, Hf, Ta, Bi, Th, U r_{Al-Si} = 0.4–0.69: TiO$_2$, Na$_2$O, Ga, Se, Cd, W, Pb, REY r_{Al-Si} = 0.2–0.39: Be, Cr, Se, Zr r_{Al-Si} < 0.2: MgO, CaO, MnO, Fe$_2$O$_3$, Co, Ni, Cu, Zn, As, Mo, Sb, Hg, Tl

Correlation with carbonate
r_{Ca} > 0.7: MgO (0.98) **, MnO (0.86) **, Ni (0.77) ** r_{Ca} = 0.5–0.69: Co (0.53), Mo (0.60) *, r_{Ca} = 0.35–0.69: As (0.49)

Correlation with sulfur
r_s > 0.7: Fe$_2$O$_3$ (0.79) **, Co (0.87) **, As (0.89) **, Hg (0.96) **, Tl (0.97) ** $r_{pyritic\ sulfur}$ >0.7: MnO (0.81) **, Ni (0.82) **, As (0.79) **, Mo (0.74) ** $r_{pyritic\ sulfur}$ = 0.5–0.69: MgO (0.60) *, CaO (0.67) *, Co (0.63) *, Hg(0.60) * $r_{pyritic\ sulfur}$ = 0.35–0.49: Tl (0.47) $r_{sulfate\ sulfur}$ > 0.7: Tl (0.81) ** $r_{sulfate\ sulfur}$ = 0.5–0.69: Hg (0.69) ** $r_{sulfate\ sulfur}$ = 0.35–0.49: Co (0.46), As (0.46) $r_{organic\ sulfur}$ > 0.7: Hg (0.80) **, Tl (0.87) ** $r_{organic\ sulfur}$ = 0.5–0.69: Co (0.66) *, As (0.60) *

Correlation with phosphate
r_P > 0.7: Li (0.91) **, F (0.91) **, Sc (0.89) **, Rb (0.79) **, Sr (0.73) **, Cs (0.76) **, In (0.77) **, Ba (0.92) **, Bi (0.85) **, Th (0.74) ** r_P = 0.5–0.69: V (0.55), Ga (0.55), Nb (0.68) *, Cd (0.50), Hf (0.64) *, Pb (0.67) *, U (0.68) * r_P = 0.35–0.49: Be (0.39), Cr (0.35), Zr (0.39), W (0.48)

Correlation coefficients between selected elements
Li: Li-Na$_2$O (0.77) **, Li-P$_2$O$_5$ (0.91) **, Li-TiO$_2$ (0.60) *, Li-K$_2$O (0.86) **, Li-F (0.96) **, Li-Ga (0.64) *, Li-Sr (0.52), Li-Ba (0.93) **, Li-Hf (0.68) *, Li-Ta (0.75) **, Li-Th (0.69) **, Li-U (0.72) **   Zr: Zr-Rb (0.63), Zr-Cd (0.94), Zr-Hf (0.85)   Be: Be-TiO$_2$ (0.86), Be-Sr (0.48), Be-Ba (0.44)   Sr: Sr-P$_2$O$_5$ (0.73) **, Sr-TiO$_2$ (0.64)*, Sr-F (0.64) *, Sr-Ba (0.73) **, Sr-Ta (0.62) *, Sr-Hf (0.61) *, Sr-Th (0.75) **, Sr-U (0.56) *   Ba: Ba-TiO$_2$ (0.78) *, Ba-Na$_2$O (0.60), Ba-K$_2$O (0.82) **, Ba-F (0.94) *, Ba-Ga (0.60) *, Ba-Hf (0.74) **, Ba-Ta (0.87) **, Ba-Th (0.87) **   Tl: Tl-Fe$_2$O$_3$ (0.74), Tl-As (0.86) **, Tl-Hg (0.98) **   Hg: Hg-Co (0.81) **, Hg-Fe$_2$O$_3$ (0.66), Hg-As (0.91) **   Ga: Ga-K$_2$O (0.69) **, Ga-F(0.63) **, Ga-Rb (0.85) **, Ga-Zr (0.86) **, Ga-Nb (0.64) *, Ga-Cs (0.87) **, Ga-Cd (0.89) **, Ga-Hf (0.85) **, Ga-U (0.89) **   F: F-Na$_2$O (0.73) **, F-K$_2$O (0.82) **, F-P$_2$O$_5$ (0.91) **, F-Rb (0.88) **, F-Nb (0.66) *, F-In (0.80) **, F-Hf (0.94) **, F-Ta (0.73) **, F-Th (0.72) **, F-U (0.75) **

** Correlation is significant at the 0.01 level (two-tailed); * Correlation is significant at the 0.05 level (two-tailed).
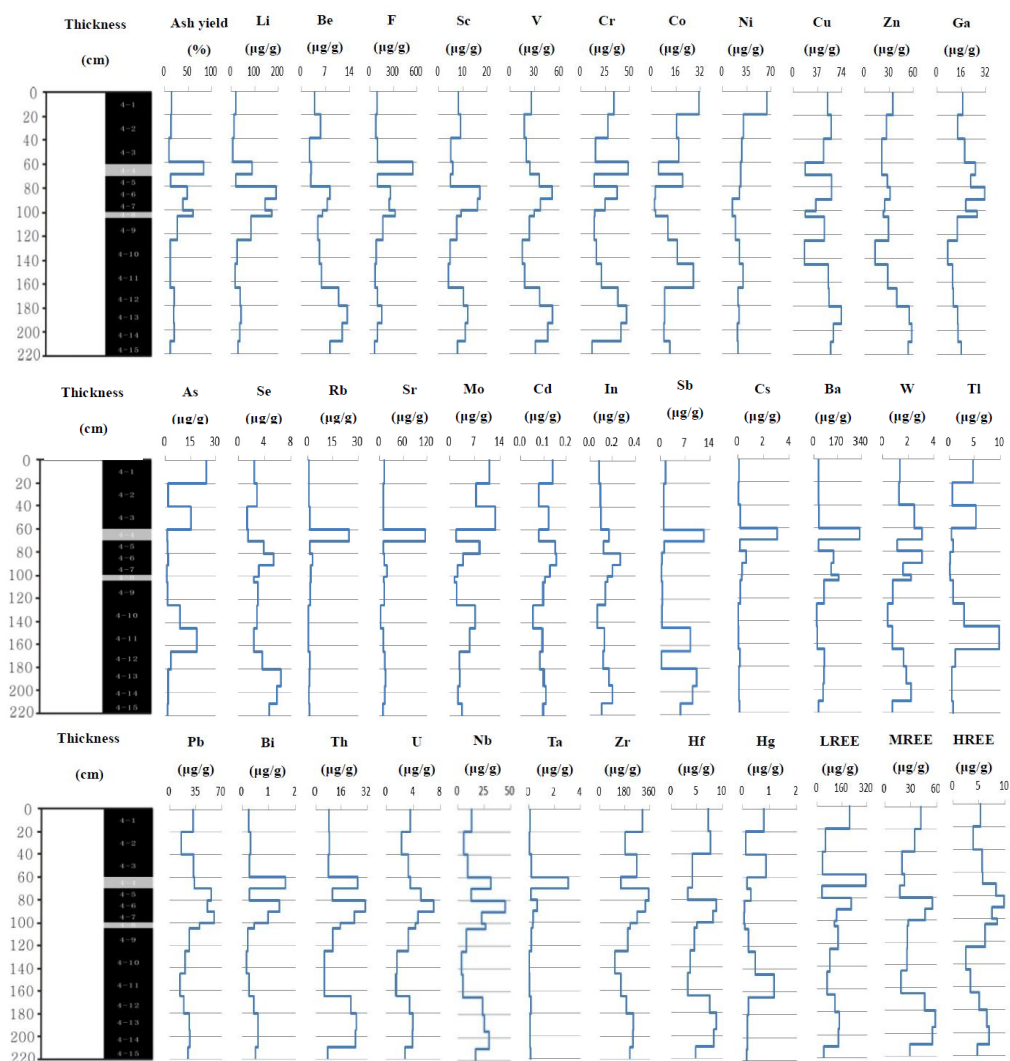
Figure 7. Concentration variations of trace elements and rare earth elements and yttrium (REY) as well as ash yield of the No. 4 coals.

Group 2 consists of TiO_2, Ga, Sr, Cd, W, Pb, and REY. These elements have a lesser but still high inorganic affinity, with correlation coefficients ranging between 0.4 and 0.69. Furthermore, all of these elements have a relatively strong affinity to Al_2O_3 and SiO_2, suggesting high affinity to silicate and aluminosilicate associations in the coals.

Group 3 includes Be, Cr, Se, and Zr, which have correlation coefficients with ash yield ranging from 0.20 to 0.39. These elements have similar correlation coefficients to ash yield as well as Al_2O_3 and SiO_2, which suggest aluminosilicate affinity.

Group 4 includes MgO, Cu, and Zn. Among these elements, MgO has high correlation coefficients with CaO and pyritic sulfur, indicating that MgO probably occurs in carbonate minerals and pyrite. Moreover, Cu and Zn both have inorganic and organic affinity, expressed by slightly weak correlation with ash yield.

Group 5 includes Fe_2O_3, CaO, MnO, Ni, Cu, Co, Ni, As, Mo, Sb, Hg, and Tl. Stibium is associated with the organic matters, which is due to its negative correlation with ash yield. In addition, MnO, Ni, Mo, Co, and As occur in carbonate minerals, demonstrated by high affinity to CaO. Furthermore, Ni, As, Mo, Co, Hg, and Tl are positively correlated with pyritic sulfur. Arsenic, Hg, Co, and Tl have high correlation coefficients with either sulfate or organic sulfur. In summary, these elements are combined with pyritic, sulfate and organic sulfur in coals.

5.2. Selected Elements

5.2.1. TiO$_2$ and Al$_2$O$_3$

Aluminum and Ti are regarded as essentially immobile elements due to their low solubility of oxides and hydroxides in low temperature aqueous solutions [47]. Therefore, the ratios between Al$_2$O$_3$ and TiO$_2$ should be close to the characteristics of their parent rocks [47,48]. The different ratios of Al$_2$O$_3$/TiO$_2$ represent different types of parent rocks. Ratios of Al$_2$O$_3$/TiO$_2$ ranging from 3 to 8 indicate mafic source rocks, 8–21 for intermediate source rocks, and 21–70 for felsic igneous rocks [47–52]. The ratio of the No. 4 coal seam samples ranges from 4.36 to 44.50 (18.96 on average), indicating that the sediments of the parent rocks have felsic or intermediate geochemical characteristics.

5.2.2. Zirconium

The concentration of Zr (235 µg/g) is significantly higher than World hard coals (36 µg/g) [41] and Chinese coals (89.50 µg/g) [20]. Zircon is generally thought to be the main mode of occurrence of Zr in most coals [50,53,54]. In studied area, the positive correlation coefficient of Zr-ash (r = 0.36), Zr-Al$_2$O$_3$ (r = 0.35) and Zr-SiO$_2$ (r = 0.39) display that kaolinite may contain Zr but is not high. In addition, Zr has also partly occurs in gorceixite and goyazite, expressed by correlation with P$_2$O$_5$ (r = 0.39), Sr (r = 0.45) and Ba (r = 0.40).

5.2.3. Beryllium

Compared to Chinese coals (2.11 µg/g) [20] and World hard coals (2 µg/g) [41], Be (6.94 µg/g) is enriched in No. 4 coals. Many scholars have stated that beryllium has organic and clay mineral associations in most coals [50,54]. In No. 4 coals, Be has positive correlation with ash yield (r = 0.31), which indicates that Be has inorganic affinity. The high correlation coefficient for Be-TiO$_2$ (r = 0.86), but low correlation coefficients for Be-Al$_2$O$_3$ (0.19) and Be-SiO$_2$ (0.36), suggest that Be is mainly associated with anatase and to a lesser extent, with clay minerals.

5.2.4. Strontium and Ba

Both Sr and Ba show significantly positive correlation with the ash yield (r$_{ash}$ = 0.60 and 0.97, respectively), indicating an inorganic association. Strontium and Ba have high correlations with Al$_2$O$_3$ (r = 0.52 and 0.92, respectively) and SiO$_2$ (r = 0.64 and 0.98, respectively), which point to aluminosilicate affinity (mainly in clay minerals) [45]. Moreover, the correlation coefficients of Sr-P$_2$O$_5$ (r = 0.73) and Ba-P$_2$O$_5$ (r = 0.92) display that gorceixite and goyazite may also be the carrier of Sr and Ba. In addition, both of Sr and Ba have high correlation coefficients with TiO$_2$ (r = 0.64 and 0.78, respectively), indicating that Sr and Ba may also occur in anatase. In terms of geochemical properties, Sr/Ba can reflect the sedimentary environment of coal formation. The average Sr/Ba ratio can represent marine sediment (r > 1) and terrestrial sediment (r < 1) [15]. In the studied area, the ratios of Sr and Ba range from 0.09 to 0.37 (0.21 on average), suggesting a terrestrial sedimentary environment.

5.2.5. Lithium

Compared to average Chinese coals [20] and world hard coals [41], Li is relatively enriched in No. 4 coal samples (52.11 µg/g on average). It should be noted that Li concentrations in the partings (132.30 µg/g on average) are typically higher than those of coal benches. Li is positively correlated with ash yield (r = 0.99), Al$_2$O$_3$ (r = 0.99), and SiO$_2$ (r = 0.97), suggesting that Li is associated with silicate and aluminosilicate minerals (mainly as kaolinite) [50]. In previous studies, the supply of sediment to the Datong Coalfield has been determined to originate from the Yinshan Oldland, located to the north of the studied area, which is mainly composed of moyite with an enrichment of Li. This is most likely the dominant source of Li [51]. In addition, the high correlation coefficients of Li-P$_2$O$_5$ (r = 0.91), Li-Sr (r = 0.52) and Li-Ba (r = 0.93) point to that Li may partly has association with gorceixite and goyazite.

Furthermore, the high correlation coefficient of Li-TiO_2 shows that anatase may also be the carrier of Li. In No. 4 coals, Li largely occurs in kaolinite, followed by anatase, gorceixite and goyazite.

5.2.6. Thallium and Hg

Compared to both average Chinese coal [20] and world hard coal [41], Tl is relatively enriched in the No. 4 coal (2.17 µg/g on average). Moreover, Hg (0.37 µg/g on average) has a higher concentration than that in both Chinese coals (0.16 µg/g) [20] and world hard coals (0.10 µg/g) [41]. Thallium and Hg are negatively associated with ash yield, indicating that they occur in organic matter in the coal. Furthermore, the correlation coefficients of Tl-S_p (r = 0.47) and Hg-S_p (r = 0.60) indicate that Tl and Hg occur as sulfide minerals (pyrite) in the coal. In addition, Tl and Hg have high correlation coefficients with sulfate (r = 0.81 and 0.69, respectively) and organic sulfur (r = 0.87 and 0.80, respectively) [51,52].

5.2.7. Gallium

The Yongdingzhuang coals have a higher Ga (15.75 µg/g) concentration than Chinese coals (6.55 µg/g) [20] and world hard coals (6 µg/g) [41]. Gallium may predominantly occur as inorganic matter in coals (r_{Ga-ash} = 0.62). Due to its similar geochemical characteristics with Al, Ga could isomorphously substitute for Al in Al-bearing minerals [33,36]. Therefore, kaolinite is the main carrier of Ga, based on the positive correlation between Ga-Al_2O_3 (r = 0.63) and Ga-SiO_2 (r = 0.62) [53]. Additionally, the correlation coefficients of Ga-P_2O_5 (r = 0.55), Ga-Sr (r = 0.33) and Ga-Ba (r = 0.60) point to that gorceixite and goyazite may also incorporate a small proportion of Ga.

5.2.8. Fluorine

The concentration of fluorine in No. 4 coals (123.54 µg/g on average) is higher than that in Chinese coals (130 µg/g) [20] and world hard coals (80 µg/g) [41]. The high correlation coefficient between F and ash yield (r = 0.96) indicates an inorganic affinity. Fluorine is significantly positively correlated with Al_2O_3 (r = 0.95) and SiO_2 (r = 0.95), indicating a close relationship between F and kaolinite. Additionally, the correlation coefficients of F-P_2O_5 (r = 0.91), F-Sr (r = 0.64), and F-Ba (r = 0.94) indicate that F also occurs in gorceixite and goyazite [36,51]. Moreover, F is positively correlated with TiO_2 (r = 0.58), which is suggestive that anatase is also one of the carriers of F. And thus, F largrly occurs in kaolinite and to a lesser extent, in anatase, gorceixite and goyazite.

5.3. Rare Earth Elements and Yttrium

5.3.1. Geochemical Characteristics of REY

The REY concentration in these coals ranges from 57.74 to 282.78 µg/g (149.09 µg/g on average), much higher than both average Chinese coal (135.89 µg/g) [20] and world hard coal (68.27 µg/g) [41]. The parting samples YDZ4-4 (339.88 µg/g) and YDZ4-8 (144.76 µg/g) have relatively higher concentrations than the other samples. In general, the REY concentration in the coal bench samples underlying partings (YDZ4-4) is higher than other samples, which are probably due to leaching, as previously reported by Crowley et al. [55] and Dai et al. [40]. However, the REY concentration of parting (YDZ4-8) is lower than that of the underlying and overlying coal benches.

Based on Seredin-Dai's classification [56], the REY were divided into three types: light (L-REY including La, La, Ce, Pr, Nd, and Sm), medium (M-REY including, Eu, Gd, Tb, Dy, and Y), and heavy (H-REY including, Ho, Er, Tm, Yb, and Lu). The concentration of LREY (34.4–219.25 µg/g, 92.65 µg/g on average) is much higher than that of MREY (16.76–58.51 µg/g, 31.25 µg/g on average) and HREY (3.15–8.85 µg/g, 5.32 µg/g on average) (Table 5). In the studied area, the correlation coefficient between REY and ash yield (r = 0.68) indicates that REY may occur as inorganic matter in coals. Additionally, the correlation coefficients of REY-Al_2O_3 (r = 0.58), REY-SiO_2 (r = 0.70), and REY-P_2O_5 (r = 0.65) suggest that REY occur in silicate and aluminosilicate or phosphate minerals.

Table 5. Concentration and geochemical parameters of REY in No. 4 coal (on whole-coal basis).

Elements	YDZ4-1	YDZ4-2	YDZ4-3	YDZ4-4	YDZ4-5	YDZ4-6	YDZ4-7	YDZ4-8	YDZ4-9	YDZ4-10	YDZ4-11	YDZ4-12	YDZ4-13	YDZ4-14	YDZ4-15	AVE
La	55.30	11.60	7.94	100.00	7.35	56.10	28.20	28.00	36.90	16.40	15.90	26.70	30.30	28.70	8.66	25.39
Ce	94.00	22.80	13.90	146.00	12.20	104.00	58.20	58.60	62.70	34.40	30.70	56.20	67.50	64.40	19.80	49.29
Pr	11.10	2.89	1.82	16.70	1.66	11.00	6.88	5.39	6.59	4.81	3.16	6.31	8.43	7.54	2.35	5.73
Nd	42.40	12.60	8.49	44.60	7.11	39.80	26.40	18.10	24.60	21.70	12.00	22.30	30.20	29.40	9.49	22.04
Sm	7.31	2.72	2.25	6.26	2.03	8.35	6.09	3.17	4.04	4.41	2.29	4.41	6.00	5.87	2.11	4.45
Eu	1.40	0.50	0.44	0.67	0.42	1.33	1.14	0.57	0.73	0.88	0.44	0.88	1.18	1.18	0.51	0.85
Gd	6.64	2.89	2.29	4.13	2.07	7.47	5.30	3.05	3.69	3.54	2.23	4.20	5.49	5.64	2.31	4.14
Td	1.01	0.60	0.43	0.56	0.38	1.35	1.11	0.64	0.65	0.60	0.37	0.82	1.12	1.09	0.46	0.77
Dy	5.55	4.29	2.56	2.87	2.29	7.23	6.05	3.41	3.43	3.36	2.29	4.85	5.92	5.86	2.92	4.35
Y	27.00	25.80	13.50	14.00	11.60	37.30	32.80	18.80	17.00	16.70	12.80	35.00	44.80	40.90	22.10	25.95
Ho	0.93	0.91	0.51	0.53	0.43	1.32	1.14	0.70	0.66	0.51	0.43	0.93	1.27	1.18	0.60	0.83
Er	2.77	2.87	1.49	1.52	1.15	3.26	2.97	1.88	1.66	1.47	1.19	2.97	3.22	3.13	1.76	2.30
Tm	0.42	0.52	0.30	0.25	0.19	0.59	0.54	0.31	0.29	0.24	0.19	0.46	0.57	0.53	0.31	0.40
Yb	2.71	2.94	1.57	1.59	1.21	3.23	3.07	1.92	1.67	1.29	1.20	2.69	3.28	3.03	1.77	2.28
Lu	0.38	0.45	0.25	0.20	0.17	0.45	0.40	0.22	0.22	0.20	0.16	0.41	0.45	0.44	0.28	0.33
$\sum$LREY	210.11	52.61	34.4	313.56	30.35	219.25	125.77	113.26	134.83	81.72	64.05	115.92	142.43	135.91	42.41	92.65
$\sum$MREY	41.6	34.08	19.22	22.23	16.76	54.68	46.4	26.47	25.5	25.08	18.13	45.75	58.51	54.67	28.3	31.25
$\sum$HREY	7.21	7.69	4.12	4.09	3.15	8.85	8.12	5.03	4.5	3.71	3.17	7.46	8.79	8.31	4.72	5.32
$\sum$REY	258.92	94.38	57.74	339.88	50.26	282.78	180.29	144.76	164.83	110.49	85.36	169.13	209.72	198.89	75.43	149.09
δCe	0.86	0.90	0.83	0.80	0.80	0.95	0.95	1.08	0.91	0.88	0.98	0.99	0.96	1.00	1.00	0.92
δEu	0.99	0.79	0.89	0.62	0.97	0.78	0.88	0.81	0.88	1.03	0.94	0.93	0.91	0.93	1.04	0.92
La_N/Sm_N	1.13	0.64	0.53	2.40	0.54	1.01	0.69	1.32	1.37	0.56	1.04	0.91	0.76	0.73	0.62	0.81
Gd_N/Lu_N	1.49	0.55	0.77	1.76	1.02	1.41	1.12	1.15	1.43	1.52	1.15	0.86	1.04	1.08	0.70	1.09
La_N/Lu_N	1.57	0.28	0.34	5.39	0.46	1.34	0.75	1.34	1.81	0.89	1.04	0.70	0.72	0.70	0.33	0.84
Type	L	H	H	L	M-H	L	M-H	L	L	M-H	L	H	M-H	M-H	H	-

N. values normalized by the average REY concentration of Upper Continental Crust. δCe = Ce_N/Ce_N * = $2Ce_N/(La_N + Pr_N)$ [57]. δEu = Eu_N/Eu_N * = $Eu_N/(0.67 \times Sm_N + 0.33 \times Tb_N)$ [58].

5.3.2. Patterns of REY

In general, to investigate the fractionation of REY concentrations in coal, the REY should be normalized by standard materials that have similar origins to coal [55,56]. As a result, it is advisable to use the UCC (Upper Continental Crust) as the standard reference for normalization rather than chondrite [56–58].

All of the coal samples are characterized by no pronounced or weak negative Ce anomalies ($\delta Ce = Ce_N/Ce_N$ * ranging from 0.78 to 1.0, average of 0.92) [58] and no pronounced and weak negative Eu anomalies ($\delta Eu = Eu_N/Eu_N$ * ranging from 0.80 to 1.04, average of 0.92) (Figure 8) [59]. Three types of coal benches were identified: L-type (L-REY; $La_N/Lu_N > 1$), M-type (MREY; $La_N/Sm_N < 1$, $Gd_N/Lu_N > 1$), and H-type (H-REY; $La_N/Lu_N < 1$) [56].
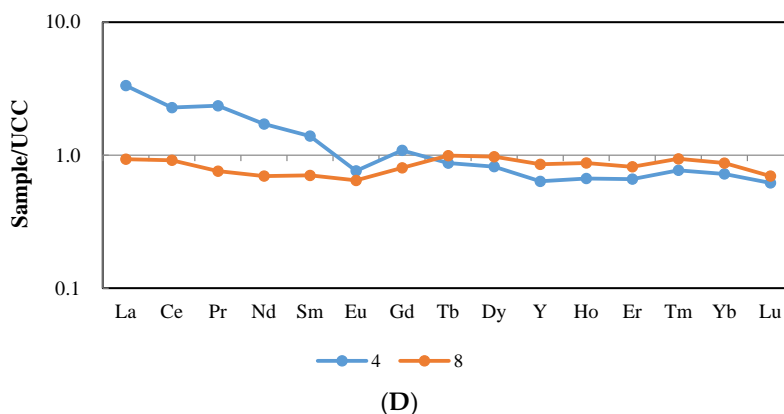
(**A**)

(**B**)

(**C**)

Figure 8. *Cont.*

(D)
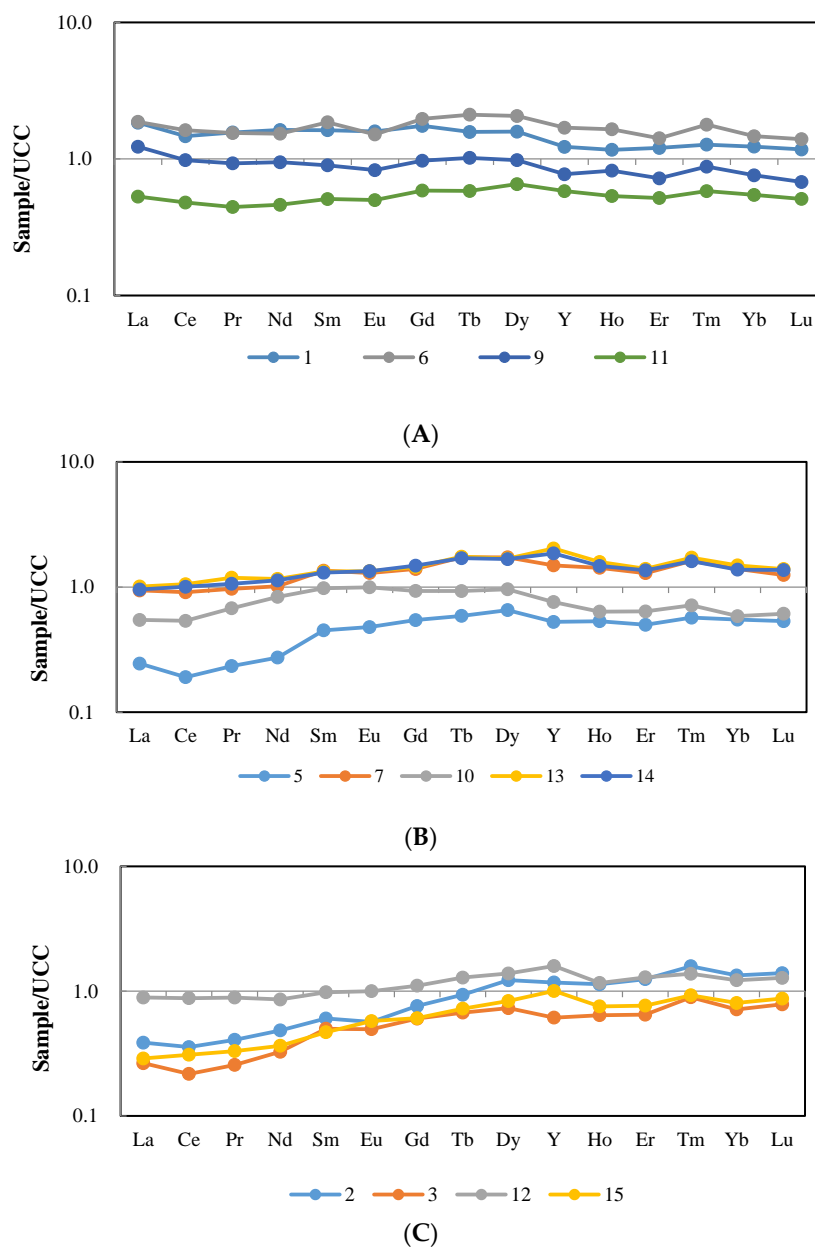
Figure 8. REY distribution patterns in the coal and partings, normalized to the upper continental crust (UCC); (A) pattern of LREE in coals; (**B**) pattern of MREE in coals; (**C**) pattern of HREE in coals; (**D**) pattern of LREE in partings.

The REY enrichment patterns can be characterized as H-type in most coal benches (YDZ4-2, YDZ4-3, YDZ4-12, and YDZ4-15). Coal samples with similar distribution patterns include YDZ4-5, YDZ4-7, YDZ4-10, YDZ4-13, and YDZ4-14 and can be characterized as M-H type enrichment. The remaining coal samples are characterized as L-type enrichment as well as two partings (YDZ4-4 and YDZ4-8). The L-type enrichment generally reflects a terrigenous origin [56]. The H-type enrichment is probably due to the injection of hydrothermal solutions, while the M-type is possibly related to natural waters [56]

In the parting sample YDZ4-8, Ce shows a slight positive Ce anomaly (δCe = 1.08) with a low concentration of REE, which is due to groundwater leaching [40,55]. Cerium is the only rare earth element that can be oxidized to Ce^{4+} and could have been precipitated in-situ, leading to high Ce and low REE concentration [51].

Dai showed that positive Eu anomalies could be caused by over estimation of Eu during the ICP-MS analysis due to interference from BaO or BaOH [58]. If Ba/Eu is > 1000, the interfered Eu is highly elevated. This indicates that when samples contain Ba/Eu less than 1000, the interference of Ba on Eu can be ignored [60]. Although No. 4 coals have high correlation coefficient between Ba and Eu (r = 0.60), low Ba/Eu value (24.50–108.77, 71.16 on average) may indicate that Eu anomalies in these samples are not caused by the interference of Ba.

As previously reported, coals with input of felsic or felsic-intermediate terrigenous materials usually display distinct negative Eu anomalies [58]. Furthermore, the ratio of Al_2O_3/TiO_2 (18.96 on average) also indicates that the input of the No. 4 coals is felsic or felsic-intermediate terrigenous materials. And thus, the Eu in No. 4 coal would be expected to have negative anomalies because the sediment source region is mainly of felsic to intermediate materials [58]. The partings (including YDZ4-4 and YDZ 4-8) have negative Eu anomalies with L-type enrichment, indicating that partings originated from felsic or felsic-intermediate terrigenous materials [56,58]. The coal bench samples, including YDZ4-1, YDZ4-6, YDZ4-9 and YDZ4-11, have no pronounced or weak negative Eu anomalis with L-type enrichment, which is due to that the input of the coals mainly originated from felsic or felsic-intermediate terrigenous materials and to a lesser extent, from mafic terrigenous materials [56,58,61]. This may be due to that the mafic terrigenous materials are characterized by positive Eu anomalies which overprinted the negative Eu negative anomalies caused by input of the felsic or felsic-intermediate terrigenous materials [56,58,61]. In addition, the samples include YDZ4-2, YDZ4-3, YDZ4-5, YDZ4-7, YDZ4-10, YDZ4-12, YDZ4-13, YDZ4-14, and YDZ4-15, showing no pronounced or weak negative Eu anomalies with H- and M-H type enrichment. In these samples, Eu dispalys no pronounced or weakly negative anomalies, probably due to the injection of

hydrothermal solutions that is characterized by positive Eu anomalies, which overprinted the negative Eu anomalies inherited from the terrigenous materials of the sediment source region [56,58,62].

In conclusion, the REY originated from the felsic or felsic-intermediate terrigenous materials (granite of Yinshan Oldland), and the natural waters or hydrothermal solutions that may circulate in coal basins [61–63].

6. Conclusions

The geochemical and mineralogical characteristics of the coal seam No. 4 of the Yongdingzhuang Mine are summarized below:

(1)　The No. 4 coal samples of the Yongdingzhuang Mine have a medium ash yield content (average 20.76%), a low moisture content (average 1.46%), a medium-high volatile content (average 27.45%), and a low sulfur content (average 0.70%).

(2)　The mineralogical compositions are mainly kaolinite and quartz with minor amounts of pyrite and anatase. Kaolinite occurs in the form of infillings in fusinite and disseminations in collodetrinite, suggesting syngenetic and early diagenetic authigenic origin. In addition, quartz occurs primarily as detrital grains derived from the source region.

(3)　The ratio of Al_2O_3 and TiO_2 in coal seam No. 4 ranged from 4.36 to 44.50 (18.96 on average), indicating that sediments formed by weathering of the parent rocks, which mainly had felsic or intermediate geochemical characteristics. The ratio of Sr and Ba ranged from 0.09 to 0.37 (0.21 on average), clearly suggesting a terrestrial sedimentary environment.

(4)　Compared to both average Chinese coals and average world hard coals, REY in the No. 4 coal seam have higher concentration. The REY mainly occurs as inorganic matter in the ash yield, which is consistent with its strong correlation with ash yield. Furthermore, no pronounced or negative Ce anomalies and weak negative or positive Eu anomalies demonstrate that the REY originated from granite of Yinshan Oldland and natural waters or hydrothermal solutions that may circulate in coal basins.

(5)　Al_2O_3 and SiO_2 are prevailing abundant major oxides in No. 4 coals, with higher SiO_2/Al_2O_3 (1.54), compared to average Chinese coals, with a large proportion of SiO_2 in the form of free silica within coals. With regard to valuable elements, the concentrations of Al, Li, Ga, Zr, Nb, Ta, Hf, Th, and REY were slightly higher than those of average world hard coals. In some coal seams, the concentrations of these elements reached industrial levels and are thus economical to extract. Furthermore, As, Hg, Be, F, U, Pb, Se, Cr, Cd, Ni, and Tl are the main hazardous trace elements in No. 4 coals. Moreover, the Be, Tl, Hg and Pb are slightly higher than in average world hard coals, which is a concern for human and environmental health during combustion and utilization. In terms of the mode of occurrence, Li, F, Cr, Ga, Se, Cd, Zr, Pb, Nb, Ta, and Hf occur as inorganic matter in clay minerals. Cobalt, Ni, As, Tl, and Hg have a strong correlation with sulfur, suggesting a occurrence in sulfide minerals. Lithium and F also occur in anatase, gorceixite and goyazite. Beryllium has affinity to anatase; gallium is mainly associated with kaolinite and to a lesser extent, with gorceixite and goyazite; zirconium also occurs as inorganic matter in ncluding kaolinie, gorceixite and goyazite. These elements and minerals should be further investigated in future studies.

References

1. BP. *BP Statistical Review of World Energy June 2014*; BP: London, UK, 2014.
2. Dai, S.F.; Finkelman, R.B. Coal geology in China: An overview. *Int. Geol. Rev.* **2018**, *60*, 531–534. [CrossRef]
3. Tian, H.Z.; Lu, L.; Hao, J.M.; Gao, J.J.; Cheng, K.; Liu, K.Y.; Qin, P.P.; Zhu, C.Y. A review of key hazardous trace elements in Chinese coals: Abundance, occurrence, behavior during coal combustion and their environmental impacts. *Energy Fuels* **2013**, *27*, 601–614. [CrossRef]
4. Tang, S.H.; Sun, S.L.; Qin, Y.; Jiang, Y.F.; Wang, W.F. Distribution characteristics of sulfur and the main harmful trace elements in China's Coal. *Acta Geol. Sin. Engl. Ed.* **2008**, *82*, 722–730.
5. Hower, J.C.; Rimmer, S.M.; Bland, A.E. Geochemistry of the blue gem coal bed, Knox County, Kentucky. *Int. J. Coal Geol.* **1991**, *18*, 211–231. [CrossRef]
6. Kolker, A.; Finkelman, R.B. Potentially hazardous elements in coal: Modes of occurrence and summary of concentration data for coal components. *Coal Prep.* **1998**, *19*, 133–157. [CrossRef]
7. Dai, S.F.; Yang, J.Y.; Ward, C.R.; Hower, J.C.; Liu, H.D.; Garrison, T.M.; French, D.; O'Keefe, J.M.K. Geochemical and mineralogical evidence for a coal-hosted uranium deposit in the Yili Basin, Xinjiang, northwestern China. *Ore Geol. Rev.* **2015**, *70*, 1–30. [CrossRef]
8. Dai, S.F.; Zeng, R.S.; Sun, Y.Z. Enrichment of arsenic, antimony, mercury, and thallium in a Late Permian anthracite from Xingren, Guizhou, Southwest China. *Int. J. Coal Geol.* **2006**, *66*, 217–226. [CrossRef]
9. Kolker, A.; Senior, C.; van Alphen, C.; Koenig, A.; Geboy, N. Mercury and trace element distribution in density separates of a South African Highveld (#4) coal: Implications for mercury reduction and preparation of export coal. *Int. J. Coal Geol.* **2017**, *170*, 7–13.
10. Seredin, V.V.; Dai, S.F.; Sun, Y.Z.; Chekryzhov, I.Y. Coal deposits as promising sources of rare metals for alternative power. *Appl. Geochem.* **2013**, *31*, 1–11. [CrossRef]
11. Dai, S.F.; Finkelman, R.B. Coal as a promising source of critical elements: Progress and future prospects. *Int. J. Coal Geol.* **2018**, *186*, 155–164. [CrossRef]
12. Dai, S.F.; Yan, X.Y.; Ward, C.R.; Hower, J.C.; Wang, X.B.; Zhao, L.; Ren, D.Y.; Finkelman, R.B. Valuable elements in Chinese coals: A review. *Int. Geol. Rev.* **2018**, *60*, 590–620. [CrossRef]
13. Dai, S.F.; Ward, C.R.; Granham, I.T.; French, D.; Hower, J.C.; Zhao, L.; Wang, X.B. Altered volcanic ashes in coal and coal-bearing sequences: A review of their nature and significance. *Earth Sci. Rev.* **2017**, *175*, 44–74. [CrossRef]
14. Dai, S.F.; Chekryzhov, I.Y.; Seredin, V.V.; Nechaev, V.P.; Granham, I.T.; Hower, J.C.; Ward, C.R.; Ren, D.Y.; Wang, X.B. Metalliferous coal deposits in East Asia (Primorye of Russia and South China): A review of geodynamic controls and styles of mineralization. *Gondwana Res.* **2016**, *29*, 60–82. [CrossRef]
15. Wang, A. Discriminant effect of sedimentary environment by the Sr/Ba ratio of different existing forms. *Acta Sedimentol. Sin.* **1996**, *3*, 297–304.
16. Dai, S.F.; Wang, P.P.; Ward, C.R.; Tang, Y.G.; Song, X.L.; Jiang, J.H.; Hower, J.C.; Li, T.J.; Seredin, V.V.; Wagner, N.J.; et al. Elemental and mineralogical anomalies in the coal-hosted Ge ore deposit of Lincang, Yunnan, southwestern China: Key role of N_2–CO_2-mixed hydrothermal solutions. *Int. J. Coal Geol.* **2015**, *152*, 19–46. [CrossRef]
17. Hower, J.C.; Granite, E.J.; Mayfield, D.B.; Lewis, A.S.; Finkelman, R.B. Notes on contributions to the science of rare earth element enrichment in coal and coal combustion by-products. *Minerals* **2016**, *6*, 32. [CrossRef]
18. Dou, G.M. *Datong Coalfield Carboniferous-Permian Coal Seam Occurrence Characteristics and Control Effects*; Taiyuan University of Technology: Taiyuan, China, 2013; (In Chinese with English abstract).
19. Liu, B.J.; Lin, M.Y. Enrichment mechanism of lithium in coal seam No. 9 of the Pingshuo mining district, Ningwu coalfield. *Geol. Explor.* **2014**, *50*, 1070–1075, (In Chinese with English abstract).
20. Dai, S.F.; Ren, D.Y.; Chou, C.-L.; Finkelman, R.B.; Seredin, V.V.; Zhou, Y.P. Geochemistry of trace elements in Chinese coals: A review of abundances, genetic types, impacts on human health, and industrial utilization. *Int. J. Coal Geol.* **2012**, *94*, 3–21. [CrossRef]
21. Liu, D.N.; Zhou, A.C.; Chang, Z.G. Geochemistry characteristics of major and rare earth elements in No. 8 raw and weathered coal from Taiyuan Formation of Datong Coalfield. *J. China Coal Soc.* **2015**, *40*, 422–430, (In Chinese with English abstract).
22. Liu, D.N.; Zhou, A.C.; Ma, M.L. Coal facies characteristics of No. 5 coal seam in Baidong Mine Area, Datong Coalfield. *Coal Geol. China* **2011**, *23*, 1–4, (In Chinese with English abstract).

23. China Coal Research Institute. *GB/T 482-2008. Sampling of Coal Seams*; Chinese National Standard; General Administration of Quality Supervision, Inspection and Quarantine of the People's Republic of China: Beijing, China, 2008. (In Chinese)

24. Dai, S.F.; Wang, X.B.; Zhou, Y.P.; Hower, J.C.; Li, D.H.; Chen, W.M.; Zhu, X.W.; Zou, J.H. Chemical and mineralogical compositions of silicic, mafic, and alkali tonsteins in the Late Permian coals from the Songzao Coalfield, Chongqing, Southwest China. *Chem. Geol.* **2011**, *282*, 29–44. [CrossRef]

25. Li, X.; Dai, S.F.; Zhang, W.G.; Li, T.; Zheng, X.; Chen, W.M. Determination of As and Se in coal and coal combustion products using closed vessel microwave digestion and collision/reaction cell technology (CCT) of inductively coupled plasma mass spectrometry (ICP-MS). *Int. J. Coal Geol.* **2014**, *124*, 1–4. [CrossRef]

26. ASTM. *Standard Test Method for Total Fluorine in Coal and Coke by Pyrohydrolytic Extraction and Ion Selective Electrode or Ion Chromatograph Methods*; Standard D5987-96, 2002; ASTM International: West Conshohocken, PA, USA, reapproved 2007.

27. Dai, S.F.; Hower, J.C.; Ward, C.R.; Guo, W.M.; Song, H.J.; O'Keefe, J.M.K.; Xie, P.P.; Hood, M.M.; Yan, X.Y. Elements and phosphorus minerals in the middle Jurassic inertinite-rich coals of the Muli Coalfield on the Tibetan Plateau. *Int. J. Coal Geol.* **2015**, *144*, 23–47. [CrossRef]

28. China Coal Research Institute. *GB/T 15224.1-2010, Classification for Quality of Coal, Part 1*; General Administration of Quality Supervision, Inspection and Quarantine of the People's Republic of China: Beijing, China, 2011. (In Chinese)

29. China Coal Science Research Institute. *MT/T850-2000, Classification for Total Moisture in Coal*; Chinese National Standard; General Administration of Quality Supervision, Inspection and Quarantine of the People's Republic of China: Beijing, China, 2000. (In Chinese)

30. China Coal Research Institute. *MT/T849-2000, Classification for Volatile Matter of Coal*; Chinese National Standard; General Administration of Quality Supervision, Inspection and Quarantine of the People's Republic of China: Beijing, China, 2000. (In Chinese)

31. China Coal Research Institute. *GB/T 15224.2-2010, Classification for Quality of Coal, Part 2*; General Administration of Quality Supervision, Inspection and Quarantine of the People's Republic of China: Beijing, China, 2011. (In Chinese)

32. Ward, C.R. Minerals in bituminous coals of the Sydney Basin (Australia) and the Illinois Basin (U.S.A.). *Int. J. Coal Geol.* **1989**, *13*, 455–479. [CrossRef]

33. Dai, S.F.; Jiang, Y.F.; Ward, C.R.; Gu, L.D.; Seredin, V.V.; Liu, H.D.; Zhou, D.; Wang, X.B.; Sun, Y.Z.; Zou, J.H.; et al. Mineralogical and geochemical compositions of the coal in the Guanbanwusu Mine, Inner Mongolia, China: Further evidence for the existence of an Al (Ga and REE) ore deposit in the Jungar Coalfield. *Int. J. Coal Geol.* **2012**, *98*, 10–40. [CrossRef]

34. Kang, J.; Li, X. Modes of occurrence of minerals in the Carboniferous coals from the Wuda Coalfield, northern China: With an emphasis on apatite formation. *Arabian J. Geosci.* **2016**, *9*, 606. [CrossRef]

35. Yang, N.; Tang, S.H.; Zhang, S.H.; Chen, Y.Y. Modes of occurrence and abundance of trace elements in Pennsylvanian coals from the Pingshuo Mine, Ningwu Coalfield, Shanxi Province, China. *Minerals* **2016**, *6*, 40. [CrossRef]

36. Dai, S.F.; Zou, J.H.; Jiang, Y.F.; Ward, C.R.; Wang, X.B.; Li, T.; Xue, W.F.; Liu, S.D.; Tian, H.M.; Sun, X.H. Mineralogical and geochemical compositions of the Pennsylvanian coal in the Adaohai Mine, Daqingshan Coalfield, Inner Mongolia, China: Modes of occurrence and origin of diaspore, gorceixite, and ammonian illite. *Int. J. Coal Geol.* **2012**, *94*, 250–270. [CrossRef]

37. Querol, X.; Chinenon, S.; Lopez-Soler, A. Iron sulphide precipitation sequence in Albian coals from the Maestrazgo basin, southeastern Iberean range, northeastern Spain. *Int. J. Coal Geol.* **1989**, *11*, 171–189. [CrossRef]

38. Dai, S.F.; Seredin, V.V.; Ward, C.R.; Hower, J.C.; Xing, Y.W.; Zhang, W.G.; Song, W.J.; Wang, P.P. Enrichment of U–Se–Mo–Re–V in coals preserved within marine carbonate successions: Geochemical and mineralogical data from the Late Permian Guiding Coalfield, Guizhou, China. *Miner. Depos.* **2015**, *50*, 159–186. [CrossRef]

39. Xiao, L.; Zhao, B.; Duan, P.P.; Shi, Z.X.; Ma, J.L.; Lin, M.Y. Geochemical characteristics of trace elements in the No. 6 Coal seam from the Chuancaogedan Mine, Jungar Coalfield, Inner Mongolia, China. *Minerals* **2016**, *6*, 28. [CrossRef]

40. Dai, S.F.; Ren, D.Y.; Chou, C.-L.; Li, S.S.; Jiang, Y.F. Mineralogy and geochemistry of the No. 6 Coal (Pennsylvanian) in the Junger Coalfield, Ordos Basin, China. *Int. J. Coal Geol.* **2006**, *66*, 253–270. [CrossRef]

41. Ketris, M.P.; Yudovich, Y.E. Estimations of clarkes for carbonaceous biolithes: World average for trace element concentrations in black shales and coals. *Int. J. Coal Geol.* **2009**, *78*, 135–148. [CrossRef]

42. Spears, D.; Zheng, Y. Geochemistry and origin of elements in some UK coals. *Int. J. Coal Geol.* **1999**, *38*, 161–179. [CrossRef]

43. Eskenazy, G.; Finkelman, R.B.; Chattarjee, S. Some considerations concerning the use of correlation coefficients and cluster analysis in interpreting coal geochemistry data. *Int. J. Coal Geol.* **2010**, *83*, 491–493. [CrossRef]

44. Kortenski, J.; Sotirov, A. Trace and major element concentration and distribution in Neogene lignite from the Sofia basin. *Int. J. Coal Geol.* **2002**, *52*, 63–82. [CrossRef]

45. Dai, S.F.; Wang, X.B.; Seredin, V.V.; Hower, J.C.; Ward, C.R.; O'Keefe, J.M.K.; Huang, W.H.; Li, T.; Li, X.; Liu, H.D. Petrology, mineralogy, and geochemistry of the Ge-rich coal from the Wulantuga Ge ore deposit, Inner Mongolia, China: New data and genetic implications. *Int. J. Coal Geol.* **2012**, *90*, 72–99. [CrossRef]

46. Yang, N.; Tang, S.H.; Zhang, S.H.; Chen, Y.Y. Mineralogical and geochemical compositions of the No. 5 Coal in Chuancaogedan Mine, Junger Coalfield, China. *Minerals* **2015**, *5*, 788–800. [CrossRef]

47. Hayashi, K.I.; Fujisawa, H.; Holland, H.D.; Ohmoto, H. Geochemistry of ~1.9 Ga sedimentary rocks from northeastern Labrador, Canada. *Geochim. Cosmochim. Acta* **1997**, *61*, 4115–4137. [CrossRef]

48. He, B.; Xu, Y.G.; Zhong, Y.T.; Guan, J.P. The Guadalupian–Lopingian boundary mudstones at Chaotian (SW China) are clastic rocks rather than acidic tuffs: Implication for a temporal coincidence between the end-Guadalupian mass extinction and the Emeishan volcanism. *Lithos* **2010**, *119*, 10–19. [CrossRef]

49. Dai, S.F.; Luo, Y.B.; Seredin, V.V.; Ward, C.R.; Hower, J.C.; Zhao, L.; Liu, S.D.; Tian, H.M.; Zou, J.H. Revisiting the late Permian coal from the Huayingshan, Sichuan, southwestern China: Enrichment and occurrence modes of minerals and trace elements. *Int. J. Coal Geol.* **2014**, *122*, 110–128. [CrossRef]

50. Finkelman, R.B. *Modes of Occurrence of Trace Elements in Coal*; U.S. Geological Survey Open-File Report No. OFR-81-99; U.S. Geological Survey: Reston, VA, USA, 1981; p. 301.

51. Dai, S.F.; Li, D.; Chou, C.-L.; Zhao, L.; Zhang, Y.; Ren, D.Y.; Ma, Y.W.; Sun, Y.Y. Mineralogy and geochemistry of boehmite-rich coals: New insights from the Haerwusu Surface Mine, Jungar Coalfield, Inner Mongolia, China. *Int. J. Coal Geol.* **2008**, *74*, 185–202. [CrossRef]

52. Duan, P.P.; Wang, W.F.; Liu, X.H.; Qian, F.C.; Sang, S.X.; Xu, S.C. Distribution of As, Hg and other trace elements in different size and density fractions of the Reshuihe high-sulfur coal, Yunnan Province, China. *Int. J. Coal Geol.* **2017**, *173*, 129–141. [CrossRef]

53. Finkelman, R.B. Trace and minor elements in coal. In *Organic Geochemistry*; Engel, M.H., Macko, S.A., Eds.; Plenum: New York, NY, USA, 1993; pp. 593–607.

54. Swaine, D.J. *Trace Elements in Coal*; Butterworths: London, UK, 1990.

55. Crowley, S.S.; Stanton, R.W.; Ryer, T.A. The effects of volcanic ash on the maceral and chemical composition of the C coal bed, Emery Coal Field, Utah. *Org. Geochem.* **1989**, *14*, 315–331. [CrossRef]

56. Seredin, V.V.; Dai, S.F. Coal deposits as potential alternative sources for lanthanides and yttrium. *Int. J. Coal Geol.* **2012**, *94*, 67–93. [CrossRef]

57. Taylor, S.R.; McLennan, S.M. *The Continental Crust: Its Composition and Evolution*; Blackwell: London, UK, 1985; p. 312.

58. Dai, S.F.; Graham, I.T.; Ward, C.R. A review of anomalous rare earth elements and yttrium in coal. *Int. J. Coal Geol.* **2016**, *159*, 82–95. [CrossRef]

59. Bau, M.; Dulski, P. Distribution of yttrium and rare-earth elements in the Penge and Kuruman iron-formations, Transvaal Supergroup, South Africa. *Precambrian Res.* **1996**, *79*, 37–55. [CrossRef]

60. Yan, X.Y.; Dai, S.F.; Graham, I.T.; He, X.; Shan, K.H.; Liu, X. Determination of Eu concentrations in coal, fly ash and sedimentary rocks using a cation exchange resin and inductively coupled plasma mass spectrometry (ICP-MS). *Int. J. Coal Geol.* **2018**, *19*, 152–156. [CrossRef]

61. Scott, C.T.; Deonarine, A.; Kolker, A.; Adams, M.; Holland, J.F. Size distribution of rare earth elements in coal ash. In Proceedings of the World of Coal Ash Conference, Nashville, TN, USA, 5–7 May 2015.

62. Hower, J.C.; Eble, C.F.; O'Keefe, J.M.K.; Dai, S.F.; Wang, P.P.; Xie, P.P.; Liu, J.J.; Ward, C.R.; French, D. Petrology, palynology, and geochemistry of Gray Hawk Coal (Early Pennsylvanian, Langsettian) in Eastern Kentucky, USA. *Minerals* **2015**, *5*, 592–622. [CrossRef]

63. Seredin, V.V. Rare earth elements in germanium-bearing coal seams of the Spetsugli Deposit (Primor'e Region, Russia). *Geol. Ore Depos.* **2005**, *47*, 238–255.